Imaging Cancer Metabolism with Positron Emission Tomography (PET)

Tim H. Witney1 and David Y. Lewis2

Abstract

Positron emission tomography (PET) enables the non-invasive spatiotemporal analysis of cancer metabolism *in vivo*. Both natural and non-natural PET tracers have been developed to assess metabolic pathways during tumorigenesis, cancer progression and metastasis. Here we describe the dynamic in vivo PET/CT imaging of the glucose analogue [^{18}F]fluoro-2-deoxy-D-glucose (FDG), taking into consideration methodology for alternative metabolic PET substrates.

Keywords: fluorodeoxyglucose, positron emission tomography, mouse

1. Introduction

Positron emission tomography non-invasively measures the uptake and retention of radiolabelled metabolites with picomolar sensitivity and sub-millimetre resolution, providing a three-dimensional view of cancer metabolism in living subjects. The most common radiolabelled metabolite is 2-[^{18}F]fluoro-2-deoxy-D-glucose (FDG), which is used as a surrogate for aerobic glycolysis, an often reported metabolic feature in cancer cells. FDG is taken up by glucose transporters, phosphorylated by hexokinase and trapped intracellularly; it cannot be further metabolised and therefore measures the rate of glucose utilisation rather than flux through the whole glycolytic pathway. FDG is used in the clinic to diagnose cancer, image invasion (staging) and monitor the effectiveness of cancer therapy (Boellaard, Delgado-Bolton et al. 2015).

To probe cancer metabolism, numerous other PET radiotracers have been developed in addition to FDG, including tracers that image fatty acid synthesis, fatty acid oxidation, oxidative stress, choline uptake and metabolism, amino acid uptake and protein synthesis rate (Lewis, Soloviev et al. 2015) (Figure 1). These radiotracers tend to be, like FDG, either fluorinated analogues which are taken up by specific mechanisms but not extensively metabolised, or cabon-11 labelled versions of endogenous substrates which are transported into the cell and metabolised via native pathways. There are advantages and disadvantages of each approach, for example, cabon-11 radiotracers require careful metabolic validation to determine what information can be obtained from the PET image, as PET provides no information of the chemical nature of the labelled metabolites. Similarly, great care needs to be taken when considering non-natural substrates as surrogates as these tracers may not reflect genuine metabolic pathway flux due to their different affinities for cognate transporters or enzymes, and retention may reflect atypical metabolism (see Note 4.1). The final choice of metabolic PET will imaging also be dictated by tracer availability (see Note 4.2).

This chapter takes you through a preclinical FDG PET/CT experiment, with special consideration given to non-standard PET tracers, where relevant, in the notes section. We describe the steps required for a successful FDG PET experiment, including PET/CT scanner, animal and radiotracer preparation; animal injection, PET/CT image acquisition, reconstruction and analysis.

2. Materials

2.1. **PET/CT scanner preparation**

2.1.1. Small animal PET/CT scanner (e.g. Mediso NanoPET/CT) with integrated heated bed and animal respiratory and temperature monitoring.

2.1.2. Phantoms and calibration sources (Hounsfield, normalisation, image quality, sodium-22 point source, 1ml syringe with 3.7MBq FDG)

2.2. Animal preparation

2.2.1. Tumour bearing mice or non-tumour bearing control mice (see Note 4.3)
2.2.2. Absorbent paper
2.2.3. Small animal heating chamber (e.g Small Warm Air System, Vet Tech).
2.2.4. Small animal heating plate (e.g. UNO Controlled Heating System).
2.2.5. Isoflurane anaesthetic machine with medical air supply via central distribution system or by pressurized tank.
2.2.6. 1 ml syringes
2.2.7. 30 G needles
2.2.8. Polyethylene tubing (0.28 mm Ø)
2.2.9. 0.9 % NaCl saline solution in water (bag of 100 mL)
2.2.10. Heparin sodium 1,000 I.U./ml solution for injection, 5mL ampoule
2.2.11. Needle forceps
2.2.12. Zinc oxide tape (1.25cm wide)
2.2.13. Animal balance
2.2.14. Infrared heat lamp
2.2.15. Topical skin adhesive

2.3. Radiotracer preparation and animal injection

2.3.1. FDG (or other metabolic PET radiotracer)
2.3.2. 5cm thick lead isotope workstation (e.g. Von Gahlen)
2.3.3. Contamination monitor (Geiger-Muller or plastic scintillator type)
2.3.4. 0.9 % NaCl saline solution in water (bag of 100 mL)
2.3.5. Heparinized saline solution (bag of 100 mL; 50 I.U./mL heparin sodium)
2.3.6. 1 ml syringes
2.3.7. Luer tip syringe caps
2.3.8. Dose calibrator
2.3.9. Isoflurane anaesthetic machine with medical air supply via central distribution system or by pressurised tank.
2.3.10. Timer

2.4. Image analysis

2.4.1. DICOM database manager
2.4.2. Image analysis software (Vivoquant, PMOD, Inveon Research Workplace, etc.)

3. Methods

3.1. PET/CT scanner preparation (prior to experiment)

3.1.1. PET/CT calibrations including Hounsfield calibration, activity calibration, normalisation and PET/CT alignment, should be performed on a regular (minimum biannually) basis in advance of the imaging study (see Note 4.4).

3.1.2. PET/CT quality control (QC) also needs to be performed regularly (recommended intervals provided in parenthesis): PET detector check (daily), Hounsfield QC (weekly), PET/CT co-registration (weekly), image quality phantom (monthly), PET activity QC with Na22 point source (weekly) and F18 syringe (monthly).

3.2. Animal preparation (the day prior to the experiment)

3.2.1. Fast animals overnight the day prior to imaging (see Note 4.5). Water must be provided *ad libitum*.

3.3. PET/CT scanner preparation (on day of experiment)

3.3.1. X-ray tube conditioning of the CT scanner (or similar, depending on make/model) should be performed on the day of imaging at least 30 minutes prior to receiving radioactivity.

3.3.2. Perform daily PET detector QC using a Na22 point source.

3.3.3. The animal bed should also be prepared in advance of receiving the radioactivity:

3.3.4. Select the correct bed for single mouse imaging (see Note 4.6).

3.3.5. Line bed with absorbent paper.

3.3.6. Heat the animal bed to 37°C.

3.3.7. Attach and position the animal breathing rate monitor and rectal temperature probe.

3.3.8. Turn on the isoflurane scavenger for the PET/CT scanner.

3.3.9. Enter the experiment and animal identification information into the study planner section of the PET acquisition software.

3.4. Animal preparation

3.4.1. Switch on and set to 37-40°C the small animal heating chamber 20-30 min prior to use.

3.4.2. Line with absorbent paper.

3.4.3. Switch on the small animal heating plate and set to 37°C.

3.4.4. Prepare anaesthesia machine by filling the isoflurane vaporiser, switching on the medical air delivery and lining the induction box with absorbent paper (see Note 4.7).

3.4.5. Prepare heparinized saline by injecting 5mL sodium heparin solution (5000 I.U.) into 100 mL bag of saline (0.9 % NaCl).

3.4.6. Injection cannulas can be prepared (one cannula per mouse) using two 30G needles and a 10-15cm length of polyethylene tubing (0.28 mm Ø). Break one needle by holding with needle forceps and twisting repeatedly until the needle breaks at the plastic end. The blunt end of this broken needle can then be placed into one end of the polyethylene tubing. The second 30G needle can then be placed needle end first into the other end of the polyethylene tubing. Finally, ensuring that no bubbles are present, fill a 1mL syringe with 200µL heparinized saline and place into the plastic port of the 30G needle (Fig 2b).

3.4.7. Bring mice to the imaging laboratory and place in heating chamber for 10-30 min prior to cannulation in order to dilute the tail vein in preparation for cannulation (see Note 4.8).

3.4.8. Attach the induction chamber to the isoflurane vaporiser and switched on. The isoflurane concentration should be set to 3% for induction of anaesthesia.

3.4.9. Once the induction chamber is filled with isoflurane, remove one mouse at a time from the heating box and place into the chamber

3.4.10. When the mouse is fully anaesthetised remove from the chamber and place on its side on the small heating plate, ensuring the nose is placed fully in the anaesthetic nose cone. Change the concentration of isofluorane to 2%.

3.4.11. Weigh and record the mouse weight by briefly transferring to an animal balance before placing back on the anaesthesia.

3.4.12. The heat lamp can also be used to ensure the mouse is warm and tail veins are fully dilated prior to inserting the cannula. Care must be taken not to place to heat lamp too close to the tail in order to prevent damage.

3.4.13. Stroke the tail moving from a proximal to distal direction to further dilate the vein. Begin cannulation attempts as distal as possible, allowing more proximal attempts as necessary.

3.4.14. To insert the cannula, grasp the mouse tail using the thumb and index finger of the non-dominant hand and bend the tail slightly so that the needle and the vein are parallel to each other (Fig 2a). Then holding the needle of the cannula in the dominant hand with the bevel up, insert the needle into the lateral tail vein of the mouse and advance the needle a few millimetres (Fig 2c). When the cannula is inserted into the vein, blood may flash back into the cannula (Fig 2d). Correct placement can be checked by flushing a small amount of saline into the vein, there will be little resistance if the cannula is in the correct place. If there is resistance and the tail around the injection site blanches white then the needle should be withdrawn and cannulation can be attempted again.

3.4.15. Once the cannula is inserted, secure it to the tail using topical skin adhesive (Fig 2d).

3.4.16. Turn on the scanner's isoflurane vaporiser, set at 2% isoflurane.

3.4.17. Transfer the animal onto the PET scanner bed. Care must be taken to support the cannula and associated syringe during transfer so it does not become dislodged.

3.4.18. Place the mouse into the scanner head-first in the prone position, ensuring the nose is placed fully in the anaesthetic nose cone. Check that the respiratory pad is positioned on the chest of the mouse.

3.4.19. Secure the mouse to the bed with a piece of tape around the midriff, tight enough to put pressure on the breathing pad and to reduce excessive movement, but loose enough to allow unrestricted respiration.

3.4.20. Secure the cannula tubing to the animal bed with tape.

3.4.21. Outstretch all of the limbs and secure these to the bed with tape.

3.4.22. Place the temperature probe into mouse rectum and secure with tape.

3.4.23. The isoflurane can be reduced to ~1% for maintenance, the depth of anaesthesia can be monitored using the respiration pads and monitoring system. The respiration rate should be maintained at about 60-100 breaths/min. If the breathing rate falls outside these limits then the concentration of isoflurane can be raised or lowered accordingly.

3.4.24. Similarly, the mouse body temperature should be maintained at 35-37°C by changing the set temperature on the animal bed as necessary.

3.4.25. Position the bed in the scanner's centre field of view using the CT's scout view by changing the bed's table height and extension into the scanner.

3.4.26. Metabolic tracers other than FDG may require different animal handling condition to those describe here for FDG (see Note 4.9)

3.5. Radiotracer preparation

3.5.1. Collect FDG from directly from supplier or temporary storage location, as F18 and C11 have short half-lives there is a necessity to work quickly.

3.5.2. Prepare radioactive doses inside a 5cm thick lead isotope workstation for radioprotection and check regularly for personal and laboratory contamination using a monitor.

3.5.3. Following FDG collection, the exact concentration of activity in MBq/mL needs to be calculated. This can be achieved by placing 100µL of the stock solution into the dose calibrator and measuring the total radioactivity. It is important to note the time of this measurement so all calculations can be decay-corrected.

3.5.4. Estimate the time of scan and using the following equation to calculate the amount of activity at the time of scan:

$$A(t) = A_0 \times e^{-\lambda t} \quad (1)$$

A(t) – radioactive dose at time t (MBq)
A(0) – original radioactive dose at time zero (MBq)

t – elapsed time from initial radioactivity measurement (min)
λ – decay constant:

$$\lambda = \frac{\ln(2)}{t_{1/2}} \quad (2)$$

$t_{1/2}$ – radioactive half-life (min); 109.7 min for F18 and 20.4 min for C11

3.5.5. From the measured stock activity, calculate the amount of activity required to make a stock solution of 18.5 MBq/ml at the time of scan. 3.7MBq is required per animal and a maximum of 10 ml/kg should be injected per mouse.

3.5.6. Once the activity doses have been calculated for 3.7 MBq of injected activity, add the exact dose volume required into a 1mL syringe, accounting for ~60 µL dead volume and place a Luer tip syringe cap on the end.

3.5.7. Using the dose calibrator, measure the syringe activity noting the time $A_1(t_1)$ (see Note 4.10).

3.6. Animal injection and PET/CT scanning

3.6.1. Under the scout view tab, drag the scan area to cover the whole mouse and conduct a scout (x-ray) scan of the mouse for positioning.

3.6.2. Using the scout view as a guideline select the PET imaging volume making sure the tumour and any other regions of interest are central to the FOV (Note 4.11).

3.6.3. For the PET acquisition parameters, set the radionuclide to F18, and the termination conditions to dynamic data collection over 90 min (Note 4.12 and 4.13).

3.6.4. Static PET imaging can also be conducted with FDG (see Note 4.14).

3.6.5. Set a timer for 15s.

3.6.6. Remove the syringe containing heparinised saline from the end of the cannula, remove the luer tip cap from the activity syringe and place it to one side. Place the activity syringe on the end of the cannula taking care not to introduce any air into the injection volume.

3.6.7. When ready, start the scan (t_0) and the timer simultaneously.

3.6.8. After 15 seconds inject the mouse with radiotracer over a period ~3 s.

3.6.9. Remove the activity syringe and replace the luer tip cap. Put the syringe containing heparinised saline back into the cannula again taking care not to introduce air and flush the cannula with 100 µL of heparinised saline.

3.6.10. Measure the remaining radioactivity within the activity syringe noting the time, $A_2(t_2)$.

3.6.11. Whilst the first scan is being performed, the next mouse can be prepared for scanning. During this 90 minutes period further mice can be cannulated and syringe radioactive doses can be drawn up and measured.

3.6.12. After the PET scan, acquire the CT over the same FOV as the PET using the following settings: same scan range as PET acquisition, helical scan, 360 projections, 55 kVp, 1100 ms exposure time (or similar depending on make and model of scanner). (Note 4.15)

3.6.13. Following CT scan, remove the dose cannula and press absorbent paper onto the mouse tail to stop bleeding.

3.6.14. Reduce the isoflurane concentration to zero and place mouse into the heated chamber for recovery, if required.

3.6.15. When mouse is freely moving around it can be put back into the home cage.

3.6.16. It may be necessary to keep the mouse in a radioactive designated area overnight, depending on the local radiation protection guidelines.

3.6.17. Alternatively, after the imaging session, place the mouse under terminal anaesthesia if tissues are required for *ex vivo* analysis (Note 4.16).

3.7. **Reconstruction**

3.7.1. Reconstruction parameters are specific to each PET scanner manufacturer and require optimisation depending on your application. For the Mediso NanoScan PET/CT we recommend dynamic Tero-Tomo 3D with the full detector model using 4 iterations and 6 subsets with 0.4 x 0.4 x 0.4 mm isotropic voxels and with decay (to the start time of the PET scan), random, attenuation and scatter correction. Using 4 x 15s, 4 x 1 min, 17 x 5 min dynamic time bins (see Note 4.17).

3.8. Image analysis

3.8.1. Reconstructed PET and CT scans can be transferred to image analysis software through a DICOM server connection. Alternatively, DICOM files can be saved on a portable storage device if a DICOM server is not available.

3.8.2. PET and CT image datasets are loaded, which should be co-registered if the PET/CT alignment has been performed correctly (see 3.1).

3.8.3. Tumour uptake can be quantified by manual drawing of regions of interest (ROI) using structural detail from the CT scanner (Note 4.18). For novel tracers, pharmacokinetics can additionally be extracted for normal tissue by placing a spherical ROI over these regions, as identified from the CT image. Muscle from the hind limb is frequently used as a measure of tracer uptake in background tissue.

3.8.4. Averaged tracer uptake across the tumour and/or tissue for each time frame should be extracted for analysis in Microsoft Excel, or similar.

3.8.5. Using equation (2) above, decay correct the original syringe radioactivity $A_1(t_1)$ and the radioactivity remaining in the syringe after injection $A_2(t_2)$ to the start time of the PET scan (t_0) (see Note 4.19). The injected dose (ID) at t_0 is then calculated:

$$ID(t_0) = A_1(t_0) - A_2(t_0) \quad (3)$$

3.8.6. The most commonly used metric for reporting PET is the standardised uptake value (SUV; Note 4.19) and this can be calculated from the region of interest using the following formula:

$$SUV(t) = \frac{C(t)}{ID(t_0)/BW} \quad (4)$$

SUV(t) – standardised uptake value at time t
C(t) – tissue radioactive concentration at time t in Bq/ml
ID (t_0) – injected dose at PET scan start time (Bq)
BW - mouse body weight (g)

3.8.7. Finally PET/CT images can be displayed, with a scale bar, using appropriate thresholds to visualise the tumour; the skeleton can be surface-rendered using Otsu thresholding to give anatomical context to the PET image (Fig 3).

4. Notes

4.1. C11 tracers have the advantage that they are "true tracers" and not analogues, therefore they follow endogenous metabolic pathways. However, this provides the added challenge that due to the lack of chemical resolution, there needs to be a careful consideration of tracer metabolism. The determination of tracer metabolism can be performed *ex vivo* using radioactive thin layer chromatography (TLC) or high performance liquid chromatography (HPLC) with radiodetection to determine the radiochemical purity. Alternatively, the metabolic species can be determined using C13 labelling as a surrogate for C11 and HPLC or gas chromatography (GC)-mass spectrometry (Lewis, Boren et al. 2014). Similarly, metabolism of F18 tracers can be followed using nuclear magnetic resonance with F19 as a surrogate. The caveat here is that C13 and F19 detection requires much higher concentrations than required for analogous detection of C11 and F18 by PET which may perturb the metabolic pathway under investigation.

4.2. In most situations PET imaging of non-standard tracers requires access to specialised radiochemistry facilities as generally only FDG (and possibly a few other metabolic tracers) are available commercially. Fluorine-18 labelled tracers have a radioactive half-life of 109.7 min and therefore can to be transported over short (>4 hour) distances. Carbon-11 has a half-life of 20.4 min so requires a nearby cyclotron facility.

4.3. The applicability and relevance of the information gained from metabolic PET imaging is proportional to the quality of the mouse model used. Where available, always use most advanced cancer models for imaging such as genetically engineered mice, patient-derived xenografts, somatic cell transduction and orthotopically implanted organoids rather than reliance on subcutaneously implanted cancer cell line models (Gengenbacher, Singhal et al. 2017).

4.4. PET scanners can only be considered accurate if calibrations and QC procedures are followed. Important calibrations include detector functioning, normalisation (to give a uniform image in the field of view despite differing sensitivity), PET/CT alignment and quantification calibration (Osborne, Kuntner et al. 2017).

4.5. Fasting mice prior to FDG PET imaging increases the tumour and reduces physiological uptake improving tumour contrast by reducing the plasma blood glucose level (Fueger, Czernin et al. 2006).

4.6. Depending on the size of the transaxial field of view, it may be possible to use a multi-mouse bed for imaging up to 4 mice simultaneously (Yagi, Arentsen et al. 2014). This can greatly improve the efficiency of PET imaging, especially for C11 studies.

4.7. Imaging requires pharmacological restraint using general anaesthesia. There have been a number of studies looking at the effects of anaesthetic and carrier gas on FDG uptake (Woo, Lee et al. , Flores, McFarland et al. 2008), the best combination to maintain high tumour and low background uptake is 0.5-1.0 % isoflurane (or sevoflurane, if available) and medical air. 100% oxygen as a carrier gas may be beneficial to maintain blood oxygen saturation in long PET experiments (>4h) or where mice are respiratory compromised such as autochthonous lung tumours bearing mice.

4.8. Mice should be pre-warmed before a PET scan and during PET imaging as this has a beneficial effect on FDG distribution, reducing physiological uptake in other organs, such as brown fat, improving the image contrast between the tumour and the background tissues (Kuntner and Stout 2014). Under anaesthesia mice are unable to regulate their core body temperature, therefore external support is required to keep the animal temperature at 37°C. External heat sources should be set to the range of 37-40°C but careful temperature monitoring using a rectal probe is required, adjusting the external heat source accordingly. There is less evidence for temperature-dependant uptake of other metabolic PET tracers, but animal heating is important for consistency, animal welfare and to preserve thermoneutral metabolism.

4.9. There is little data optimising anaesthesia and animal handling regimes for other metabolic PET tracers so careful consideration needs to be given. Additionally, there is little data for the benefits of fasting for the uptake of other tracers, it may even reduce tumour uptake in some cases. If mice are sick due to high tumour burden then fasting can push them into a torpor, which could be considered non-physiological. To be sure of the effect of any animal handling procedures (i.e. diet, anaesthesia or temperature), PET tracer uptake should be compared under the different proposed conditions.

4.10. The time recorded for the injected radioactivity dose needs to be synchronous with the time of the PET/CT scanner as these are used for decay correction and a few minutes difference can be significant particularly with C11 imaging (Boellaard 2009).

4.11. The centre of the PET field of view is the point in the PET scanner with the highest resolution and sensitivity (hence signal-to-noise ratio), therefore it is important to position the animal so that the tumour (or other region of interest) is in the centre of the scanner.

4.12. Initial PET studies with novel tracers should always be dynamic, i.e. injection and imaging of the animal throughout the uptake and distribution period. FDG is irreversible bound inside the cell so uptake should increase until a plateau, usually 60-90 min after injection. A number of metabolic PET tracers (e.g. FET, FSPG, FACBC) are reversible, therefore will wash in and out of the tumour, here the plateau phase is transient and varies between different models, therefore dynamic imaging is frequently required to determine the optimal imaging time point. Often the peak of the tumour uptake is used but the time point with maximum tumour-to-background will improve visualisation. The optimal time-point also depends on the tracer metabolism to ensure that the process of interest is dominant in the PET image (Lewis, Boren et al. 2014).

4.13. Dynamic PET data can be analysed using quantitative models, ranging in complexity from graphical methods (i.e. Patlak plot) using image-derived input functions to fully quantitative multi-compartment models using metabolite corrected arterial plasma samples. The

advantage of PET pharmacokinetic modelling is that it allows the derivation of *in vivo* flux measurements, which take into account variable tracer delivery and whole-body tracer metabolism (Kuntner and Stout 2014).

4.14. The kinetics of FDG tissue distribution are well-known, therefore static PET scans (~10 min) are often performed. Here, the animal is injected with radioactivity outside of the scanner, with imaging performed at a pre-determined time point(s) after injection. For FDG this should be a minimum of 60 min after injection. It is important to keep to a consistent imaging time, as small variations in time may result in large differences in tissue uptake of the radiotracer. Another point to consider for static scans is whether the animals are allowed to wake in-between tracer injection and scanning. This will have a large effect on tracer pharmacokinetics due to the altered metabolism, breathing and heart rates experienced during anaesthesia.

4.15. The purpose of the CT scan is three-fold, to provide anatomical context to the PET image, for PET signal attenuation correction and where possible, to localise the tumour.

4.16. If tissue needs to be collected immediately after imaging for dissection, gamma counting and other downstream analysis, CT scans can be performed prior to PET imaging.

4.17. Most manufacturers will have their own reconstruction algorithms for PET reconstruction, these can generally be separated into 2D or 3D filtered-back projection (FBP) and 2D or 3D iterative reconstruction. Generally, 3D iterative reconstruction, such as 3D-ordered subset expectation maximisation (OSEM), is preferable as it gives the best image quality. 3D iterative reconstructions have high computational demands and therefore used to have long reconstruction times. Newer reconstruction algorithms run on graphics processing units (GPU) allowing dynamic 3D reconstructions in hours rather than days.

4.18. There is less selection bias when performing region of interest analysis on the CT rather than the PET image. However, as CT soft tissue contrast is poor, visualising autochthonous and orthotopic tumours can be difficult. Here, image thresholding of the PET scan may be required (i.e. selecting all the voxels inside the tumour volume above a certain value). Due the lack of CT soft tissue contrast, MRI is a better imaging modality for tumour segmentation.

4.19. SUV is the radioactivity concentration normalised to the injected dose and the body weight and provides a semi-quantitative measure of metabolic activity. An SUV of 1 is equivalent to complete and uniform distribution of radioactive signal throughout the body. Therefore, tumour SUV >1 suggest tumour localisation and SUV is, for the most part, proportional to the glucose utilisation rate. In addition, the percentage of injected activity, normalised for the volume of the tissue or organ of interest, is frequently used for data analysis in preclinical imaging studies when body weights are broadly equivalent.

Figures

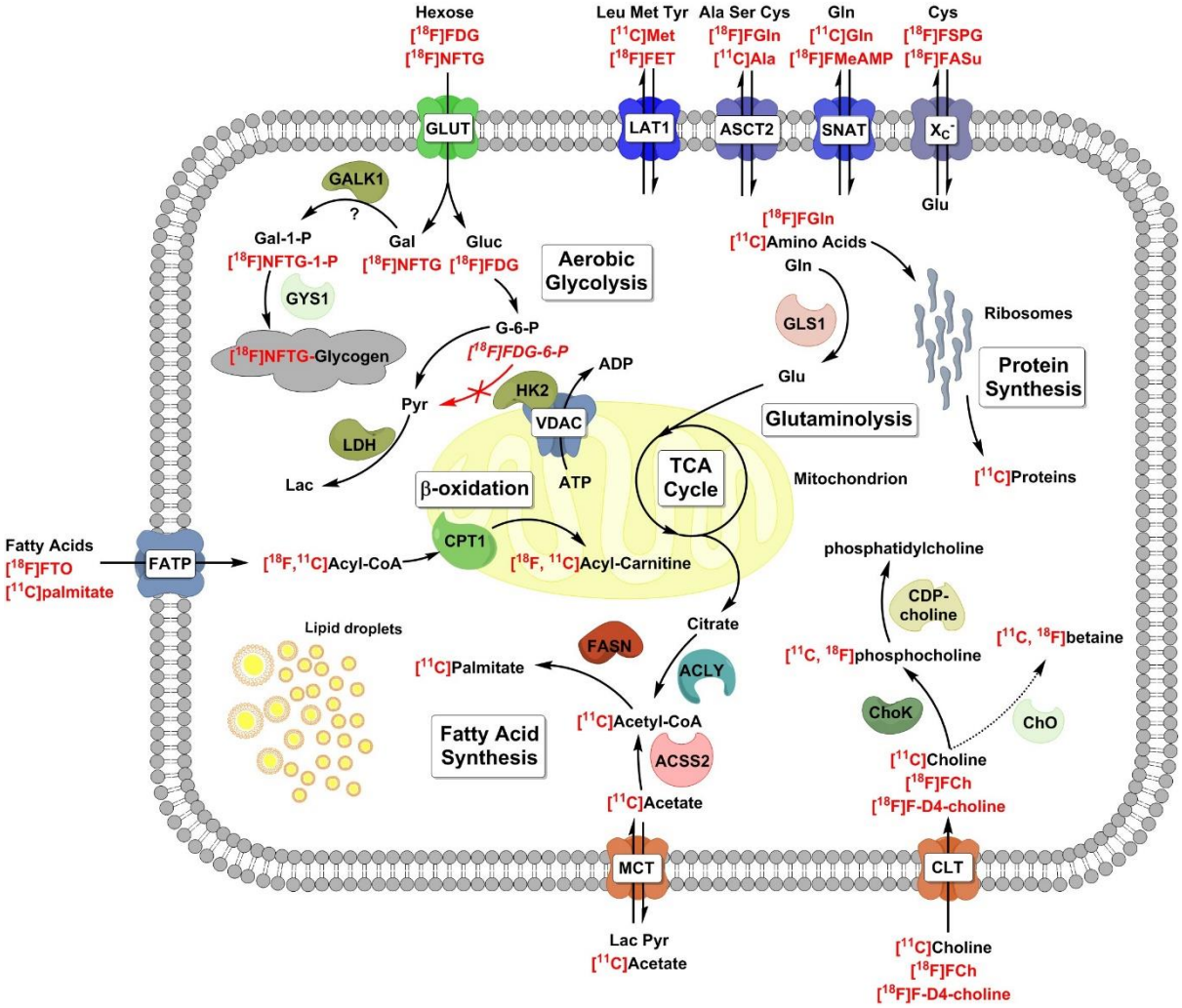

Figure 1. A schematic of the metabolic pathways and enzymes responsible for the intracellular trapping of key PET substrates for imaging cancer metabolism. Radionuclides and PET substrates are shown in red. ACLY – ATP citrate lyase; ACSS2 – acetyl coA synthetase short-chain family member 2, cytosolic; ASCT2 - neutral amino acid transporter (SLC1A5); Ala – alanine; CPT1 – carnitine palmitoyl transferase I; CTL – choline transporter–like proteins (SLC44A); Cys – cysteine; FASN – fatty acid synthase; FATP – fatty acid transport protein; Gal – galactose; GALK1 – galactokinase 1; GLS1 – glutaminase 1; Gluc – glucose; Gln – glutamine; Glu – glutamate; GLUT – glucose transporter; GYS1 – UDP-glucose-glycogen glucosyltransferase; HK2 – hexokinase 2; LAT1 - L-type amino acid transporter 1 (SLC7A5); LDH – lactate dehydrogenase; MCT monocarboxylate transporter; SNAT – system A amino acid transporter; XC− – anionic amino acid transporter light chain, system xc− (SLC7A11); TCA – tricarboxylic acid cycle; VDAC – voltage-dependent anion channel. Reproduced with permission from (Lewis, Soloviev et al. 2015)

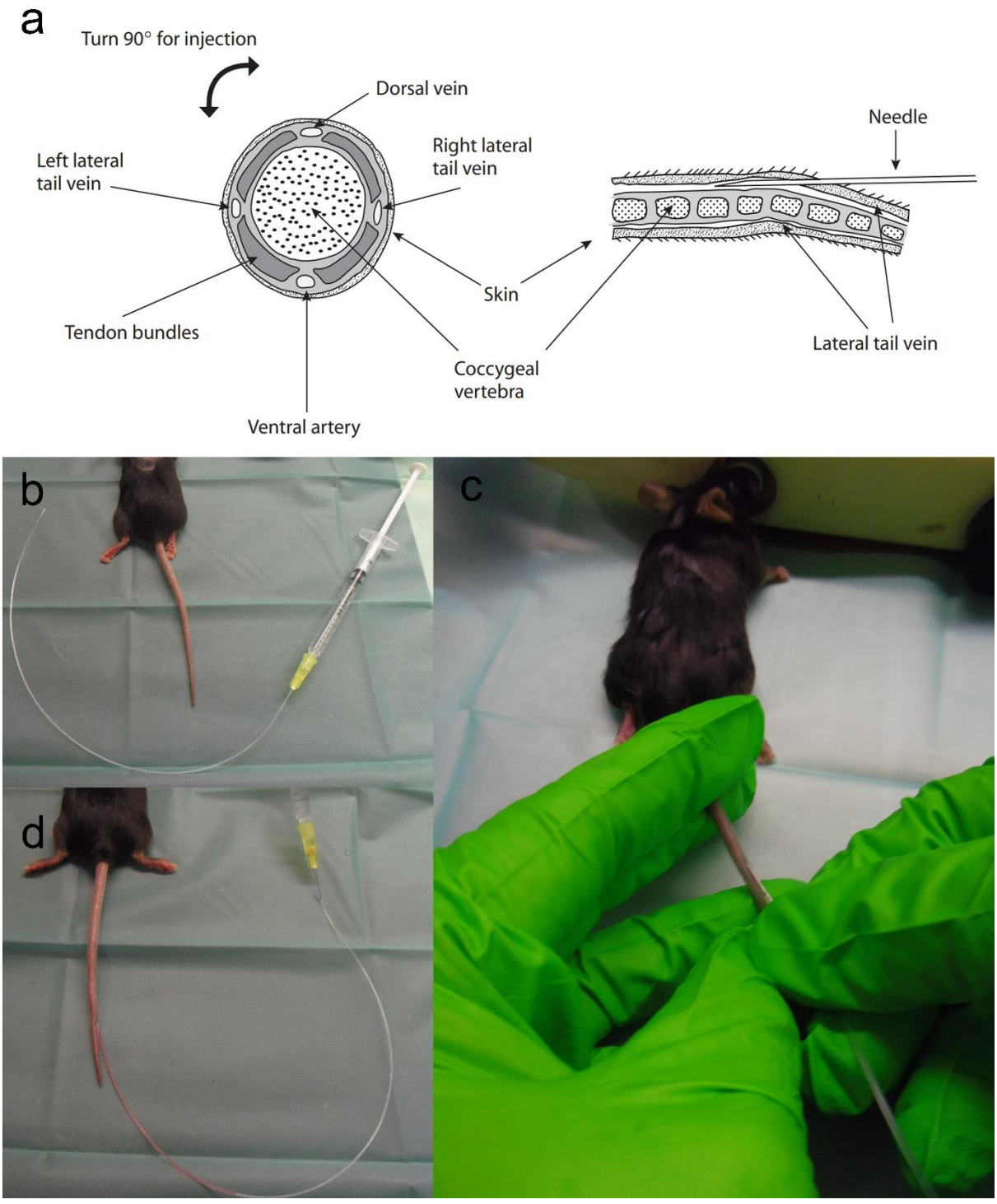

Figure 2. Mouse tail vein cannulation procedure for i.v. injection of FDG. (a) schematic of mouse tail anatomy showing path of needle insertion (Hirota and Shimizu 2012), (b) Assembled tail vein cannula, (c) cannula is inserted into the lateral tai vein, (d) cannula in place secured using tissue adhesive show blood flashback. Images courtesy of Dr De-en Hu, University of Cambridge, UK.

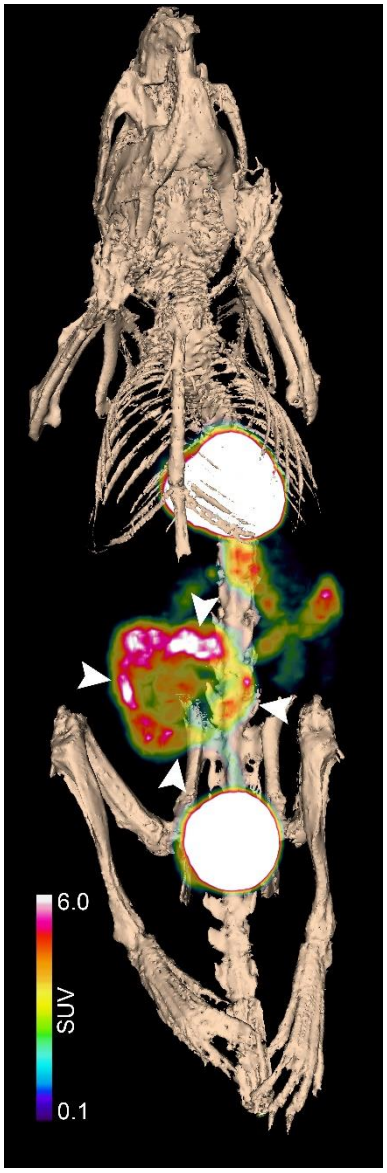

Figure 3. FDG PET/CT image of a $Kras^{G12D/+}$; $Tpr53^{R172H/+}$; Pdx-1-Cre mouse bearing a pancreatic ductal adenocarcinoma (PDAC) tumour (white arrows) with high glucose uptake. Physiological FDG uptake in the heart, bladder and kidneys can also be observed.

Boellaard, R. (2009). "Standards for PET image acquisition and quantitative data analysis." J Nucl Med **50 Suppl 1**: 11S-20S.

Boellaard, R., R. Delgado-Bolton, W. J. Oyen, F. Giammarile, K. Tatsch, W. Eschner, F. J. Verzijlbergen, S. F. Barrington, L. C. Pike, W. A. Weber, S. Stroobants, D. Delbeke, K. J. Donohoe, S. Holbrook, M. M. Graham, G. Testanera, O. S. Hoekstra, J. Zijlstra, E. Visser, C. J. Hoekstra, J. Pruim, A. Willemsen, B. Arends, J. Kotzerke, A. Bockisch, T. Beyer, A. Chiti, B. J. Krause and M. European Association of Nuclear (2015). "FDG PET/CT: EANM procedure guidelines for tumour imaging: version 2.0." Eur J Nucl Med Mol Imaging **42**(2): 328-354.

Flores, J. E., L. M. McFarland, A. Vanderbilt, A. K. Ogasawara and S. P. Williams (2008). "The effects of anesthetic agent and carrier gas on blood glucose and tissue uptake in mice undergoing dynamic FDG-PET imaging: sevoflurane and isoflurane compared in air and in oxygen." Mol Imaging Biol **10**(4): 192-200.

Fueger, B. J., J. Czernin, I. Hildebrandt, C. Tran, B. S. Halpern, D. Stout, M. E. Phelps and W. A. Weber (2006). "Impact of animal handling on the results of 18F-FDG PET studies in mice." J Nucl Med **47**(6): 999-1006.
Gengenbacher, N., M. Singhal and H. G. Augustin (2017). "Preclinical mouse solid tumour models: status quo, challenges and perspectives." Nat Rev Cancer **17**(12): 751-765.
Hirota, J. and S. Shimizu (2012). Chapter 5.2 - Routes of Administration A2 - Hedrich, Hans J. The Laboratory Mouse (Second Edition). Boston, Academic Press**:** 709-725.
Kuntner, C. and D. Stout (2014). "Quantitative preclinical PET imaging: opportunities and challenges." Frontiers in Physics **2**(12).
Lewis, D. Y., J. Boren, G. L. Shaw, R. Bielik, A. Ramos-Montoya, T. J. Larkin, C. P. Martins, D. E. Neal, D. Soloviev and K. M. Brindle (2014). "Late Imaging with [1-(11)C]Acetate Improves Detection of Tumor Fatty Acid Synthesis with PET." J Nucl Med **55**(7): 1144-1149.
Lewis, D. Y., D. Soloviev and K. M. Brindle (2015). "Imaging tumor metabolism using positron emission tomography." Cancer J **21**(2): 129-136.
Osborne, D. R., C. Kuntner, S. Berr and D. Stout (2017). "Guidance for Efficient Small Animal Imaging Quality Control." Mol Imaging Biol **19**(4): 485-498.
Woo, S.-K., T. S. Lee, K. M. Kim, J.-Y. Kim, J. H. Jung, J. H. Kang, G. J. Cheon, C. W. Choi and S. M. Lim "Anesthesia condition for ¹⁸F-FDG imaging of lung metastasis tumors using small animal PET." Nuclear Medicine and Biology **35**(1): 143-150.
Yagi, M., L. Arentsen, R. M. Shanley and S. K. Hui (2014). "High-throughput multiple-mouse imaging with micro-PET/CT for whole-skeleton assessment." Phys Med **30**(7): 849-853.